Notch Pathway Inhibition Depletes Stem-like Cells and Blocks Engraftment in Embryonal Brain Tumors

Xing Fan,[1] William Matsui,[2] Leila Khaki,[1] Duncan Stearns,[1] Jiong Chun,[3] Yue-Ming Li,[3] and Charles G. Eberhart[1,2]

Departments of [1]Pathology and [2]Oncology, Johns Hopkins University School of Medicine, Baltimore, Maryland and [3]Molecular Pharmacology and Chemistry Program, Memorial Sloan-Kettering Cancer Center, New York, New York

Abstract

The Notch signaling pathway is required in both nonneoplastic neural stem cells and embryonal brain tumors, such as medulloblastoma, which are derived from such cells. We investigated the effects of Notch pathway inhibition on medulloblastoma growth using pharmacologic inhibitors of γ-secretase. Notch blockade suppressed expression of the pathway target Hes1 and caused cell cycle exit, apoptosis, and differentiation in medulloblastoma cell lines. Interestingly, viable populations of better-differentiated cells continued to grow when Notch activation was inhibited but were unable to efficiently form soft-agar colonies or tumor xenografts, suggesting that a cell fraction required for tumor propagation had been depleted. It has recently been hypothesized that a small population of stem-like cells within brain tumors is required for the long-term propagation of neoplastic growth and that CD133 expression and Hoechst dye exclusion (side population) can be used to prospectively identify such tumor-forming cells. We found that Notch blockade reduced the CD133-positive cell fraction almost 5-fold and totally abolished the side population, suggesting that the loss of tumor-forming capacity could be due to the depletion of stem-like cells. Notch signaling levels were higher in the stem-like cell fraction, providing a potential mechanism for their increased sensitivity to inhibition of this pathway. We also observed that apoptotic rates following Notch blockade were almost 10-fold higher in primitive nestin-positive cells as compared with nestin-negative ones. Stem-like cells in brain tumors thus seem to be selectively vulnerable to agents inhibiting the Notch pathway. (Cancer Res 2006; 66(15): 7445-52)

Introduction

Medulloblastoma and other embryonal brain tumors are thought to arise primarily from neural stem/precursor cells of the ventricular zone and cerebellar external germinal layer (1–3). Pathways such as Wingless, Hedgehog, and Notch, which control the specification, proliferation, and survival of nonneoplastic neural precursors, are also all aberrantly activated in such tumors, suggesting a molecular link between neural stem cells and medulloblastoma (4–9). These developmentally significant signaling pathways are attractive therapeutic targets. For example, several groups have shown that pharmacologic inhibitors of Hh signaling block the proliferation and survival of medulloblastoma *in vitro* and *in vivo* (10–12). Such therapeutic advances are clearly needed, as current embryonal brain tumor treatments are associated with significant side effects and often do not result in cures (13–15).

In addition to arising from stem or precursor cells, medulloblastoma may also contain functionally important subsets of cells with stem-like properties. It has recently been hypothesized that in many types of cancer, including medulloblastoma, such stem-like cells are uniquely capable of propagating tumor growth (16–18). This "cancer stem cell" hypothesis is based, in part, on paradigms explaining the development and repair of normal organs, in which only stem cells are thought to have a long-term capacity for self-renewal and are therefore necessary for the generation and regeneration of tissues. Experimental support for the existence of a discrete cancer cell subpopulation required for tumor propagation initially came from clonogenic assays, which showed that only a small portion of tumor cells could form colonies *in vitro* or engraft *in vivo* (19–21). Only recently the prospective isolation of cells uniquely capable of propagating neoplasms has been achieved, providing firmer support for the presence of cancer stem cells (22, 23). This has been made possible by the characterization of markers that identify stem-like cells in tumor specimens. Two such markers, CD133 and side population, have been used to prospectively isolate a small percentage of cells in brain tumors uniquely able to generate tumor neurospheres and xenografts (24–27). Interestingly, both markers were initially identified in nonneoplastic stem cells (28–31), highlighting the similarities between normal and malignant stem cells.

To date, no agent has been shown to target the cancer stem cell subpopulation in solid tumors. However, similarities in the growth characteristics and gene expression patterns of benign neural stem cells and brain tumor stem cells suggest that the same signaling pathways may be required for survival and growth in both (18, 32–35). Notch is known to promote the survival and proliferation of nonneoplastic neural stem cells and to inhibit their differentiation (36, 37). Signaling is initiated by ligand binding, followed by intramembranous proteolytic cleavage of the Notch receptor by the γ-secretase complex. Inhibitors of this complex slow the growth of Notch-dependent tumors such as medulloblastoma and T-cell leukemia (8, 9, 38). We therefore used a potent small-molecule γ-secretase inhibitor to further investigate the role for Notch signaling in medulloblastoma, comparing the effects on overall tumor cell mass to those on cells expressing stem-like markers. Our data indicate that stem-like brain tumor cells may be especially vulnerable to attacks on molecular pathways, such as Notch, which are required in their nonneoplastic cognate cells.

Requests for reprints: Charles G. Eberhart, Department of Pathology, Johns Hopkins University School of Medicine, Ross Building 558, 720 Rutland Avenue, Baltimore, MD 21205. Phone: 410-502-5185; Fax: 410-955-9777; E-mail: ceberha@jhmi.edu.

doi:10.1158/0008-5472.CAN-06-0858

Materials and Methods

Cell culture. The DAOY, PFSK, D283Med, and D425Med cell lines were obtained from the American Type Culture Collection and maintained in MEM (Invitrogen, Carlsbad, CA) supplemented with 10% fetal bovine serum (FBS) unless otherwise noted. Cell pools and stable subclones transfected with Notch2 intracellular domain (NICD2) were generated as previously described, and, unless otherwise noted, the DAOY:NICD2 subclone used is the same as the one previously reported (8). The low-passage medulloblastoma line MB2 was derived from a tumor resected at Johns Hopkins Hospital and analyzed at passage 8 to 9. It was finely minced, triturated, and maintained in MEM with 10% FBS. For treatment studies, cells were plated and allowed to grow overnight in medium containing 10% FBS; then medium was replaced the next morning with low-serum (0.5% FBS) MEM containing γ-secretase inhibitor dissolved in DMSO at the concentrations indicated. RNA and protein extractions and all cell-based assays were done 48 hours after drug application unless otherwise noted. All experiments with error bars were done in triplicate and shown as mean values with SE unless otherwise noted. Cell mass was measured using CellTiter assays according to the instructions of the manufacturer (Promega, Madison, WI). Cell number and viability were assessed using the Guava PCA and Viacount reagent according to instructions (Guava Technologies, Heyward, CA). Soft-agar assays were done as previously described, with colonies counted using an automated reader (8).

γ-Secretase inhibitor synthesis. The potent γ-secretase inhibitor [11-*endo*]-*N*-(5,6,7,8,9,10-hexahydro-6,9-methanobenzo[*a*][8]annulen-11-yl)-thiophene-2-sulfonamide was listed as compound 18 in the recent report by Lewis et al. (39) describing its synthesis and testing, and we refer to it as GSI-18. It was synthesized as previously described (39) and its identity and quality were confirmed by nuclear magnetic resonance and mass spectral analysis. The biological activity of this inhibitor against γ-secretase was confirmed using *in vitro* and cell-based assays as previously described (40).

Immunocytochemistry. The cell lines DAOY and MB2 were seeded in 12-well tissue culture plates and allowed to adhere overnight. After treating with 2 μmol/L GSI-18 for 48 hours, cells were washed with PBS and fixed using 4% paraformaldehyde solution in PBS at room temperature for 30 minutes. Cells were then permeabilized with 0.4% Triton X-100 in PBS for 5 minutes at room temperature, washed with PBS, and incubated in 5% bovine serum albumin (BSA)-PBS for 1 hour and then in 1:1,000 anti-nestin antibody (Chemicon, Temecula, CA) or 1:500 anti–cleaved caspase-3 (Cell Signaling Technology, Beverly, MA) in 1% BSA-PBS for 2 hours. After washing with PBS, a final 60-minute incubation with a 1:300 dilution of Cy3-conjugated goat anti-mouse and Cy2-conjugated goat anti-rabbit secondary antibodies (Jackson ImmunoResearch Laboratories, West Grove, PA) diluted in PBS containing 1% BSA was done. After washing with PBS, cells were then counterstained with 4′,6-diamidino-2-phenylindole (Vector Laboratories, Burlingame, CA), mounted, and visualized with fluorescence microscope (Zeiss, Jena, Germany). In the single-immunolabeling study (Fig. 6*A* and *C*), six high-power fields of DAOY cultures containing 147 to 333 (mean, 193) cells were photographed and the percentages of cells positive for nestin were scored in a blinded fashion. In the double-immunolabeling study (Fig. 6*D-F*), 10 high-power fields were photographed and counted.

Flow cytometric analyses. Flow cytometric analysis of S-phase fraction and cell cycle kinetics was done following fixation and staining with propidium iodide using a FACSCalibur (Becton Dickinson, San Jose, CA) with CELL Quest version 3.3 software (8). CD133 studies were done using the same instrument, with antibodies from Miltenyi Biotec (Auburn, CA) according to the instructions of the manufacturer. In brief, cells were blocked in Fc receptor blocking reagent and incubated with CD133/1 (AC133)-phycoerythrin antibody (Miltenyi Biotec) for 10 minutes in the dark at 4°C. Then cells were washed and resuspended in 500 μL buffer (PBS containing 0.5% BSA and 2 mmol/L EDTA). Cells expressing levels of CD133 higher than those seen in immunoglobulin G (IgG) controls were considered positive. Experiments measuring CD133 were repeated two to three times for each line and error bars represent the mean and SD. For analyses of side population, cells (10^6/mL) were incubated with Hoechst 33342 (3 μmol/L; Molecular Probes, Carlsbad, CA) for 90 minutes at 37°C in DMEM containing 2% FBS. Before analysis, cells were washed and resuspended in 2 μg/mL propidium iodide (Sigma, St. Louis, MO). Cells were analyzed on a LSR flow cytometer equipped with 424/44-nm band pass and 670-nm long pass optical filters (Omega Optical, Brattleboro, VT). To ensure proper identification of side population cells, cells were incubated as above with the addition of 50 μmol/L verapamil (Sigma).

Real-time reverse transcription-PCR. Quantitative reverse transcription-PCR (RT-PCR) for Notch1, Notch2, and Hes1 was done as previously described (31), with all reactions normalized to actin (Applied Biosystems, Foster City, CA). Commercially available Assay on Demand TaqMan primers and probes were used to measure mRNA for Tuj1 and the α_6 subunit of the γ-aminobutyric acid type A receptor (GABRA6). Each quantitative RT-PCR reaction was done in triplicate and error bars represent SE.

Protein analysis. Western blots contained 20 μg of protein per lane on a 10% Tris-glycine SDS-PAGE gel (Invitrogen) and electrophoresing for several hours in 1× TG-SDS buffer (Amresco, Solon, OH). Proteins were transferred to 0.45-μm Optitran nitrocellulose (Schleicher & Schuell, Keene, NH) in 1× Tris-glycine buffer (Amresco). Blots were blocked in PBS containing 5% nonfat dry milk powder and incubated overnight at 4°C with antibodies directed against Hes1 (kind gift of Dr. Tetsuo Sudo, Toray Industries, Tebiro, Kamakura, Japan; 1:2,000) or glyceraldehyde-3-phosphate dehydrogenase (Research Diagnostics, Flanders, NJ; 1:20,000). Blots were then washed several times with PBS containing 0.1% Tween 20 and incubated in peroxidase-conjugated IgG diluted 1:2,000 in blocking solution. After washing several times in PBS with 0.1% Tween 20, blots were developed with enhanced chemiluminescence reagent (Pierce, Rockford, IL) and exposed to film.

Statistical analysis. Statistical analyses were done using GraphPad Prism 4 (GraphPad Software, San Diego, CA). Data graphed with error bars represent mean and SE from experiments done in triplicate unless otherwise noted. A two-sided Student's *t* test was used to determine the significance of any differences.

Results

Growth of medulloblastoma cultures is slowed but not arrested by Notch blockade. Experiments were done using GSI-18, a potent γ-secretase inhibitor with a sulfonamide core (39). We first sought to determine what concentration of GSI-18 effectively inhibited Notch activity in tumor cells by measuring expression of the pathway target Hes1. GSI-18 at 2 μmol/L reduced both mRNA and protein levels of Hes1 in DAOY cells by >70% (Fig. 1*A* and *B*), suggesting that this concentration should be sufficient to cause antitumor effects mediated by Notch pathway inhibition. GSI-18 levels <0.4 μmol/L did not affect Hes1 mRNA expression (data not shown).

Notch pathway inhibition using GSI-18 slowed the growth of DAOY medulloblastoma cultures. The increase in viable cell mass over 2 days was reduced in a dose-dependent fashion by GSI-18 (Fig. 1*C*) but many tumor cells survived Notch pathway inhibition and continued to proliferate over this period. JC2, a γ-secretase inhibitor with a benzodiazepine core, also slowed but did not arrest growth in medulloblastoma cell mass when used at concentrations that effectively inhibited the Notch pathway, indicating the findings were not specific to one structural class of compound (data not shown). DAOY cells stably transfected with a NICD2 were used to further control for the specificity of the pharmacologic effects. This truncated Notch receptor does not require ligand binding or γ-secretase activity for nuclear translocation and signaling, and cells expressing it should be insensitive to effects of GSI-18 mediated by Notch2 inhibition. NICD2 expression in a stable subclone we have previously described (8) rescued the negative effects on DAOY cell mass (Fig. 1*D*). A second stable subclone, as

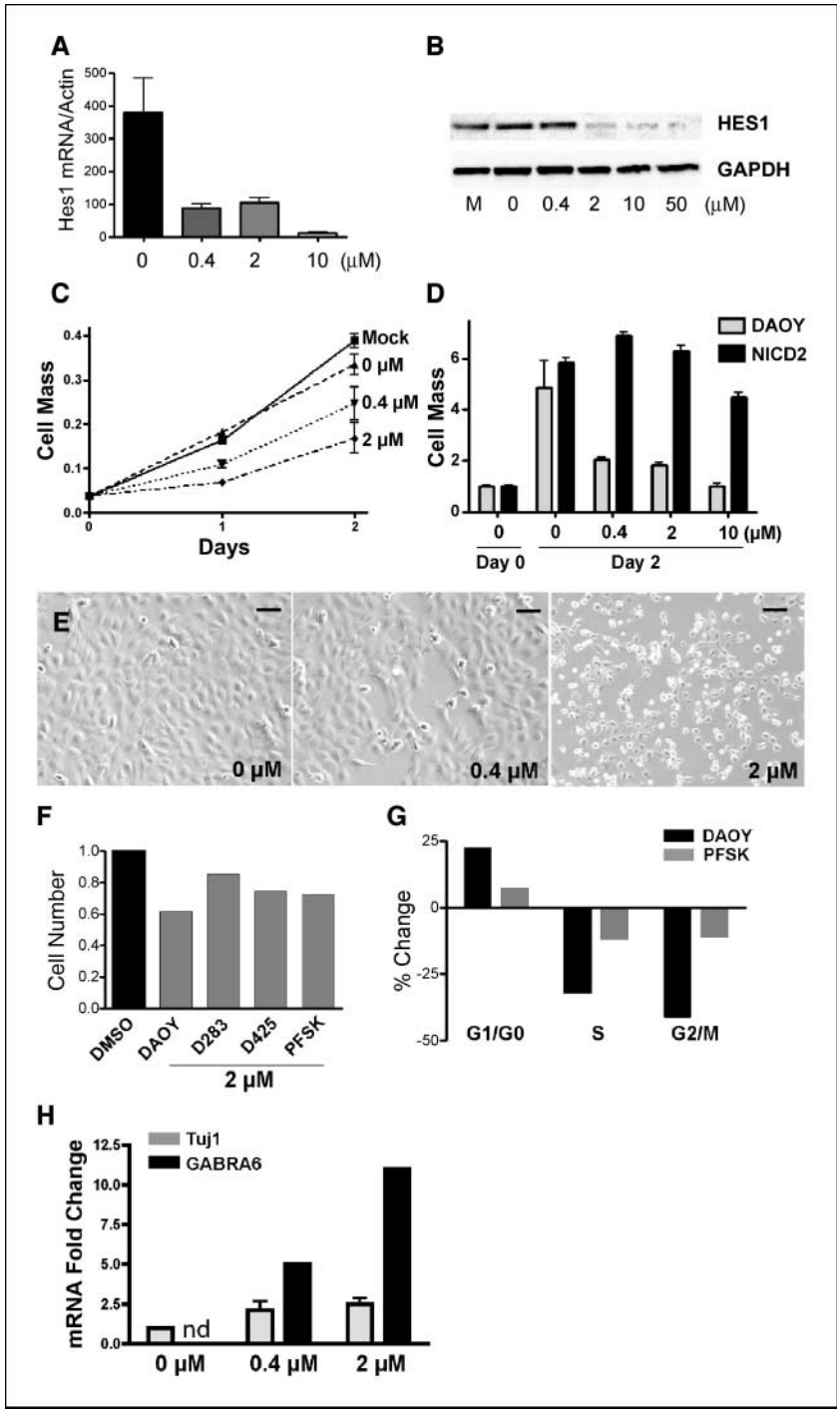

Figure 1. Notch inhibition slowed growth of embryonal brain tumor cells. *A,* Hes1 mRNA levels, measured using quantitative RT-PCR and normalized to actin expression, are decreased by 0.4 μmol/L or higher levels of GSI-18. *B,* Hes1 protein levels are also reduced after 48-hour exposure to GSI-18. *C,* growth of DAOY viable cell mass over 2 days is slowed in a dose-dependent fashion by GSI-18. *D,* NICD2 expression in a stable subclone rescues the growth inhibition caused by GSI-18. *E,* DAOY cells are less numerous and smaller after 2 days of Notch blockade; bar, 100 μm. *F,* the number of viable cells, expressed as a fraction of vehicle-treated cultures, is reduced after 48 hours of Notch pathway blockade in all four medulloblastoma/PNET cell lines tested. *G,* flow cytometric analysis of DAOY and PFSK cultures after 48 hours of 2 μmol/L GSI-18 exposure revealed increases in the percentage of cells in G_1/G_0 and decreases in the S and G_2-M fractions, graphed as percent change from cells treated with DMSO alone. *H,* expression of mRNAs encoding the neuronal markers Tuj1 and GABRA6 are induced by the γ-secretase inhibitor GSI-18; *nd,* not detected.

well as a pool of cells into which NICD2 was introduced by transfection, was also resistant to the growth-inhibiting effects of GSI-18 (data not shown), suggesting that this compound acts through Notch and not other pathways regulated by γ-secretase.

It has previously been reported that in pre-T cells, down-regulation of Notch activity reduces cellular metabolism and cell size (41). We also observed decreased cell size in medulloblastoma cultures following GSI-18 exposure (Fig. 1*E*). To rule out the possibility that our measurements of viable cell mass bioreductive capacity (CellTITER assay) were being altered by metabolic affects of Notch, we quantitated cell number using flow cytometry. The number of live cells in DAOY, D283Med, D425Med, and PFSK cultures exposed to 2 μmol/L GSI-18 for 48 hours was reduced as compared with vehicle-treated controls, but the reduction was less than that of cell mass (Fig. 1*F*). Thus, measures of both cell mass and cell number show a slowing, but not an arrest, of tumor growth under conditions of Notch blockade.

Decreased proliferation and increased neuronal differentiation following Notch inhibition. Flow cytometric analysis showed that 2 μmol/L GSI-18 increased the G_1-G_0 cell fraction and decreased the S-phase and G_2-M fractions of DAOY and PFSK cell lines (Fig. 1*G*), suggesting that cell cycle exit likely plays a role

in its antigrowth effects. Notch pathway down-regulation has also been linked to cellular differentiation in both normal development and in neoplasms (42, 43) and we therefore examined whether Notch inhibition caused cellular differentiation. γ-Secretase inhibition in DAOY cells increased RNA levels of two markers of cerebellar neuronal differentiation, Tuj1 and GABRA6, in a dose-dependent fashion (Fig. 1*H*). One of these neuronal markers, GABRA6, is specifically found in cerebellar granule cells in the brain, where its expression is induced as they mature (44). Its induction after Notch pathway inhibition suggests that the differentiation pathway being actuated resembles that in normal cerebellar granule neuron precursors, and highlights the similarities between the DAOY line and developing cerebellum.

Notch blockade by γ-secretase inhibitors suppresses tumor formation. We next examined the effects of Notch pathway blockade on tumor formation *in vitro* and *in vivo*. We first used a clonogenic assay to determine whether cells capable of forming anchorage-independent colonies were depleted by GSI-18. Vehicle-treated DAOY cultures seeded in soft agar formed 50 colonies per field on average (Fig. 2). This number dropped to 4 when an equal number of viable cells was counted and seeded after 48 hours of treatment with GSI-18 and increased to 119 in the presence of constitutive Notch2 activation. Thus, whereas many tumor cells continued to grow in 2 μmol/L GSI-18, their clonogenicity in soft agar was suppressed by >90%.

To determine the effects of Notch blockade on the formation of tumor xenografts, DAOY and DAOY:NICD2 cultures were treated with either 2 μmol/L GSI-18 in DMSO or DMSO alone, and the viable cells remaining after 48 hours were counted using trypan blue. Five hundred thousand viable cells from each group were then mixed with Matrigel and injected s.c. in athymic (nude) mice. Large xenografts formed at the sites of all 12 control injections, including vehicle-treated DAOY cells (n = 4; Fig. 3*A*), vehicle-treated DAOY:NICD2 cells (n = 4), and GSI-18-treated DAOY:NICD2 cells refractory to Notch inhibition (n = 4). In contrast, only one very small lesion formed among the four sites injected with 500,000 DAOY cells that had been pretreated with 2 μmol/L GSI-18, suggesting that while viable, the cancer cells were no longer

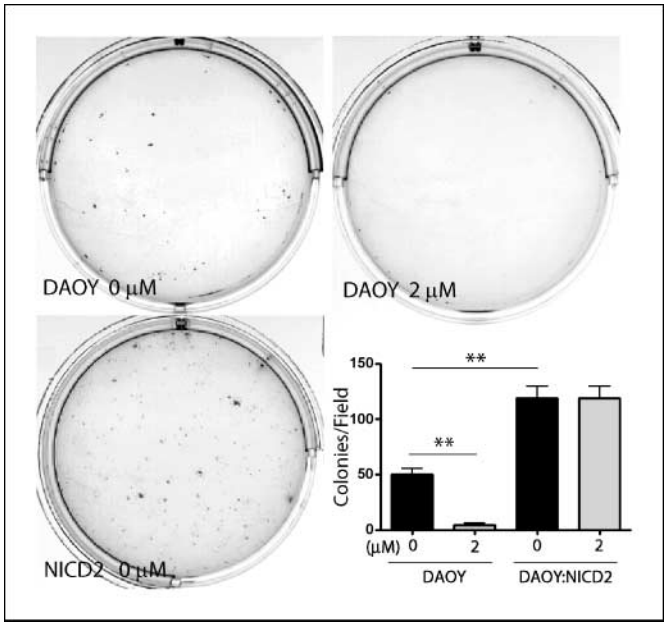

Figure 2. Notch signaling is required for the formation of colonies in soft-agar. Forty-eight hours of exposure to 2 μmol/L GSI-18 before seeding in soft agar significantly reduced clonogenic potential of DAOY cells. This effect could be rescued by NICD2 expression in a stable subclone (**, P < 0.001).

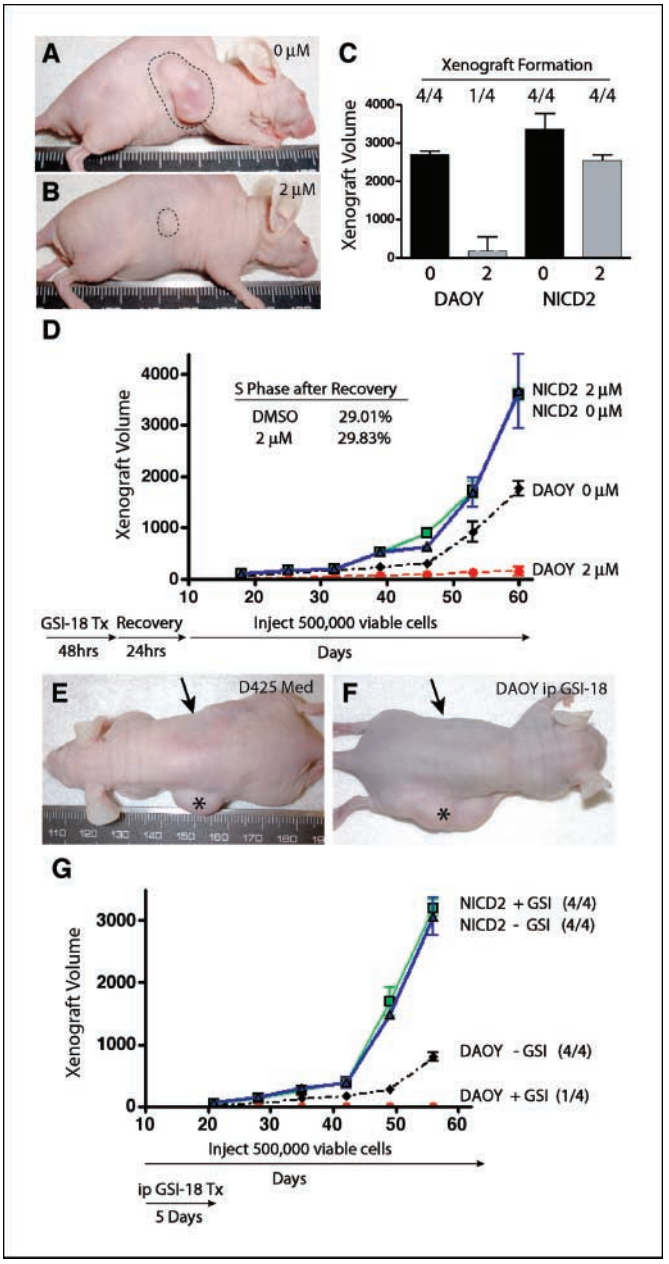

Figure 3. Notch pathway inhibition blocks xenograft formation. *A* to *C,* bulky xenografts developed at all 12 sites injected with cells in which Notch signaling was active. This included vehicle-treated DAOY (n = 4), vehicle-treated DAOY:NICD2 (n = 4), and 2 μmol/L GSI-18–treated DAOY:NICD2 (n = 4; *A*). Viable cells remaining following Notch blockade with 2 μmol/L GSI-18 formed a tumor mass (*B*) at only one of four injection sites. *D,* after recovering for 24 hours in media containing 10% FBS, GSI-18- and vehicle-treated cultures have identical proliferation rates as determined by flow cytometric analysis of S-phase fraction (*inset*). Nevertheless, cells that had experienced Notch pathway blockade were still unable to efficiently form tumors, with small lesions developing at only two of four injection sites. As before, large xenografts formed at all 12 control sites. *E,* D425Med cells treated with GSI-18 for 48 hours also failed to generate xenografts (*arrow*) whereas vehicle-treated cells always did (*asterisk*). *F* and *G, in vivo* administration of GSI-18 i.p. for 5 days after s.c. tumor injection also blocked engraftment of DAOY (*arrow*) but not of DAOY:NICD2 (*asterisk*).

tumorigenic (Fig. 3*B* and *C*). To rule out the possibility that cells were alive but moribund following γ-secretase inhibition, the experiment was repeated with cells counted after a recovery period. After 2 days of treatment, followed by 24 hours of recovery in medium containing 10% FBS and no γ-secretase inhibitor, both GSI-18-treated and vehicle-treated cells proliferated at similar rates, suggesting that any overall effects on growth had normalized (Fig. 3*D*). When equal numbers of these "recovered" cells were injected into mice, GSI-18-treated cultures were still unable to form tumors ($n = 4$) whereas bulky tumor xenografts formed in all 12 controls. D425Med and D283Med cells also failed to engraft ($n = 2$ animals D425Med, $n = 3$ animals D283Med) when pretreated for 48 hours with GSI-18, whereas vehicle-treated cells injected on the contralateral flank formed large tumors at all but one site (Fig. 3*E*).

As a test of the requirement for ongoing Notch activity during tumor engraftment, we treated animals with GSI-18 after s.c. injections of DAOY and DAOY:NICD2 cells into their left and right flanks. A treatment group of four animals received i.p. injections containing 0.5 mg GSI-18 in DMSO for 5 consecutive days, beginning on the day of xenograft initiation, whereas the control group was treated with vehicle alone. DAOY cells failed to engraft in three of the four GSI-18-treated animals whereas vehicle-treated animals all developed tumors (Fig. 3*F* and *G*). Tumors also developed in both vehicle- and GSI-18-treated animals at sites of DAOY:NICD2 injection. No behavioral or physical changes were noted in the animals treated with GSI-18.

Notch regulates the percentage of medulloblastoma cells expressing stem/precursor markers. The data presented above suggest that while viable and proliferative following Notch pathway blockade, medulloblastoma cultures are altered in some way, blocking their ability to form soft-agar colonies and tumor xenografts. It has been shown that stem-like "side-populations" in established brain tumor cell lines are uniquely able to form xenografts (25, 26). Thus, cancer stem cells seem to be able to persist in established brain tumor lines maintained for many years in culture. Because stem-like tumor cells are thought to be critical for xenograft formation, we sought to determine if this subpopulation might be especially sensitive to Notch pathway blockade.

We first examined the requirement for ongoing Notch activity in CD133-positive cells. Singh et al. (24, 33) have shown that only CD133-positive medulloblastoma and glioblastoma brain tumor cells are able to form multipotent neurosphere clones or tumor xenografts. Another type of brain tumor, ependymoma, also seems to contain a small fraction of CD133-positive cells uniquely capable of engrafting in immunocompromised mice (27). In the adherent embryonal brain tumor cell lines DAOY and PFSK, flow cytometric analysis revealed that 9.9% and 10.8% of cells, respectively, expressed CD133 on their surface (Fig. 4*A* and *B*). These CD133-positive fractions fell within the 6.1% to 45.4% range (mean, 19.7%) reported in primary medulloblastoma (33). The D283Med and D425Med lines, which have elevated c-Myc levels and grow in suspension, contained higher percentages of CD133-positive cells. Sorting of DAOY and PFSK cultures generated populations enriched ~3-fold for cells expressing CD133 and negative fractions in which <1% of cells were CD133 positive. Interestingly, mRNA levels of Hes1, a marker of Notch pathway activity, were elevated 4-fold in the CD133-enriched fraction of DAOY and 5-fold in the CD133-enriched fraction of PFSK (Fig. 4*C*). This suggests that Notch signaling is especially active in stem-like cancer cells and supports the possibility that Notch pathway inhibition may target this population.

Gain or loss of Notch pathway activity modulated the size of the CD133-expressing stem-like subpopulation (Fig. 4*B*). This fraction was elevated from 9.9% to >17% in a pool of DAOY cells transfected with a plasmid encoding the constitutively active NICD2 and in two stable subclones derived from such a pool. In contrast, Notch pathway inhibition using GSI-18 reduced the CD133-positive stem-like fraction 3-fold to 3.3% ($P < 0.01$). As expected, NICD2 expression rescued the effects of GSI-18 on the CD133-positive cell fraction. A 4.8-fold reduction in the percentage of CD133-positive cells seen in PFSK cultures was also statistically significant ($P < 0.01$). Decreases in the stem-like fraction were also observed in the D283Med and D425Med lines but were less pronounced.

Side population was analyzed to obtain a second measure of the effects of Notch on stem-like tumor cells. DAOY cultures contained a Hoechst 33342–excreting side population of 1.9% (Fig. 5*A*). The multiple drug resistance pumps mediating dye efflux are verapamil sensitive (28), and adding verapamil to the medulloblastoma culture abolished Hoechst excretion, verifying that this was a bona fide side population. Consistent with our hypothesis that Notch activity regulates stem-like cancer cells, constitutive activation of Notch2 increased the side population almost 4-fold to 7.3%, whereas Notch inhibition essentially ablated it, with only 0.01% of remaining cells negative for dye (Fig. 5*A* and *B*). NICD2 expression protected the side population from GSI-18 exposure, but not from verapamil, indicating that the effect of GSI-18 was specifically mediated through its effects on Notch signaling. Small side populations were also present in the PFSK, D283Med, and D425Med cell lines and were ablated by both verapamil (data not shown) and 2 μmol/L GSI-18 (Fig. 5*B*). Thus, Notch pathway blockade depletes the stem-like subpopulation defined either by CD133 or by side population.

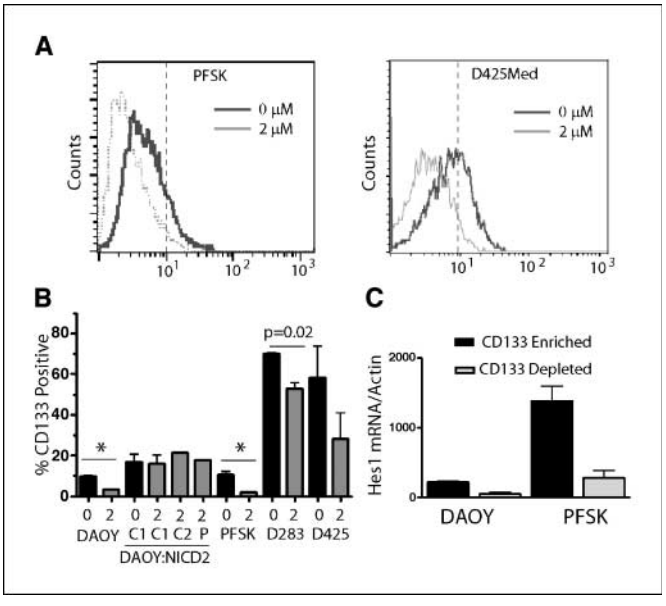

Figure 4. The CD133-positive population in medulloblastoma is regulated by Notch. *A,* flow cytometric analysis was used to define the population of cells with CD133 expression elevated above the highest level of background fluorescence (*dashed line*). Cultures were evaluated following 48-hour exposure to either 2 μmol/L GSI-18 or vehicle. *B,* the CD133-positive subpopulation in all four medulloblastoma/PNET lines examined was reduced by 2 μmol/L GSI-18 (*, $P < 0.01$). Constitutive activation of Notch2 in a pool of DAOY cells transfected with NICD2 (*P*) as well as in two stable subclones (*C1* and *C2*) rendered the CD133-expressing subpopulation insensitive to γ-secretase inhibitor. *C,* Hes1 mRNA levels were elevated in CD133-enriched preparations as compared with CD133-depleted ones, suggesting Notch activity is higher in stem-like cells.

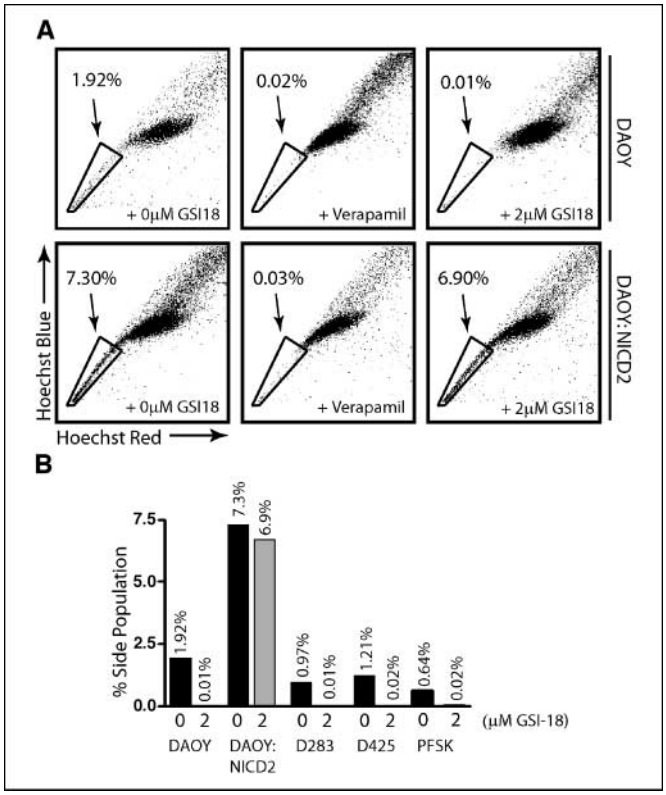

Figure 5. Notch blockade ablates side population. *A,* a verapamil-sensitive side population is present in DAOY cultures and is ablated by GSI-18 treatment. NICD2 expression in a stable subclone increases the size of the side population almost 4-fold and rescues the effects of the γ-secretase inhibitor. *B,* similar effects are seen in PFSK, D283Med, and D425Med medulloblastoma lines.

Notch blockade induces apoptosis in nestin-positive medulloblastoma cells. We next examined if stem or progenitor-like cells expressing nestin might be especially prone to apoptosis following Notch pathway blockade. Expression of the intermediate filament nestin was used to directly visualize poorly differentiated cells, as CD133 immunofluorescence was too dim to reliably score by eye. Nestin mRNA levels were not significantly elevated in CD133-enriched DAOY populations, suggesting that the two markers are not equivalent (data not shown). This is not unexpected, as Lee et al. (45) also found that only 20% of CD133-positive cells in the postnatal cerebellum also expressed nestin. Nevertheless, nestin was one of the first markers of neural stem cells to be identified (46) and its expression has been shown in a subset of cells within neurospheres derived from primary human medulloblastoma, suggesting it marks stem-like cells in these tumors (32, 33). We detected nestin protein in both established (DAOY) and low-passage (MB2) medulloblastoma cultures. Nestin staining was present in the cytoplasm and was variable in intensity, with only 10% of DAOY cells expressing high levels whereas almost half of MB2 cells were strongly nestin positive (Fig. 6*A* and *B*). We reasoned that medulloblastoma cells expressing high levels of nestin might represent a stem-like subpopulation and we therefore correlated their percentage with varying levels of Notch activity. In DAOY cells, constitutive Notch2 activation up-regulated the strongly nestin-positive fraction of cells almost 5-fold to 47.7% ($P < 0.001$) whereas Notch blockade using the γ-secretase inhibitor GSI-18 reduced this population 4-fold to 2.4% ($P < 0.01$; Fig. 6*C*). A significant reduction was also observed in MB2 cells following Notch blockade.

We used double immunofluorescence to study cell death in medulloblastoma cells positive or negative for nestin. The basal apoptotic rate was measured using antibodies specific for cleaved caspase-3. In DAOY cultures to which vehicle was added for 48 hours, the apoptotic rate was low in both nestin-negative (26 of 1,841; 1.4%) and nestin-positive (4 of 160; 2.5%) cells (Fig. 6*D-F*). However, after 48 hours of treatment with 2 μmol/L GSI-18, the apoptotic rate increased to 37% in the nestin-positive population (23 of 62 cells) whereas apoptosis in the better-differentiated cells lacking nestin only increased to 3.9% (40 of 1,017 cells). Interestingly, nestin was less evenly distributed in the apoptotic cells and was sometimes observed surrounding the degenerating nuclei. Such cagelike perinuclear nestin staining has been previously described in mitotic cells (47). Our immunofluorescent assessment of cell death using cleaved caspase-3 corresponds relatively well to apoptotic induction measured by flow cytometric analysis of Annexin staining, suggesting that our manual counting procedure is accurate (Fig. 6*G*). Taken together, these data indicate that the survival of stem-like tumor cells is more sensitive to Notch pathway inhibition than the survival of better-differentiated cells.

Discussion

In this study, we examined the effects of Notch pathway inhibition on the growth and xenograft formation of medulloblastoma. We found that Notch blockade using the γ-secretase inhibitor GSI-18 slowed the growth of tumor cells *in vitro* but had a much more dramatic effect on the formation of colonies in soft agar and tumor xenografts in nude mice. Indeed, our most striking finding was that large numbers of viable, rapidly proliferating cells were not able to generate bulky xenografts if they had previously been treated with GSI-18, whereas equal numbers of vehicle-treated cells always formed large tumors. Systemic (i.p.) treatment of animals with GSI-18 also blocked xenograft formation with no apparent side effects, indicating this agent may be effective therapeutically in preventing tumor metastasis or regrowth following debulking. We believe that these dramatic effects on tumor propagation are mediated by depletion of cancer stem cells, as subpopulations expressing the stem cell marker CD133, as well as the stem-like side population, were profoundly reduced by Notch blockade. These results must be extended to primary tumors or additional low-passage lines and might provide a first indication that stem-like cells can be successfully ablated from brain tumors.

The targeted depletion of stem-like cells we observe following Notch pathway blockade contrasts sharply with prior reports of cancer stem cell survival following standard chemotherapies. For example, Wulf et al. (48) showed higher efflux of chemotherapeutic agents and better survival in leukemic side population cells as compared with non-side population cells. Based on this and on similar studies, it has been suggested that the efflux pumps which define side population also function to remove toxic chemotherapy drugs from cancer stem cells (reviewed in refs. 49, 50). In support of this concept, treatment of neuroblastoma cell lines with mitoxantrone actually increases the side population, suggesting that stem-like cancer cells are relatively resistant to this chemotherapeutic agent and accumulate as more differentiated cells are killed (51). Thus, conventional chemotherapies effectively remove the better-differentiated cells while leaving most stem-like cells alive. In contrast, Notch blockade depletes stem-like cells but leaves many better-differentiated cells capable of limited growth intact.

We examined only one type of malignant brain tumor in this study, but our findings may be applicable to other neoplasms as well. The Notch pathway is known to regulate stem cells in a wide variety of tissues and Notch blockade seems to affect survival and proliferation of multiple types of cancer (52, 53). For example, Notch is activated by translocation or mutation in >50% of T-cell acute lymphoblastic leukemia, and anti-Notch therapies have been shown to slow acute lymphoblastic leukemia growth *in vitro* (38). Aberrantly activated Notch signaling has also been documented in lung, breast, salivary gland, and pancreatic carcinoma (54–57). γ-Secretase inhibitors may therefore be useful in targeting stem-like cancer cells in a wide range of neoplasms.

In the future, multiagent chemotherapeutic regimens may target both stem-like and better-differentiated cells. Drugs blocking Notch signaling, or other pathways required in stem cells such as Wnt and Hedgehog, will be used to deplete the cancer stem cell population, and traditional chemotherapeutic agents can be used at the same time to debulk the larger mass of tumor cells. This will effect a rapid removal of both subpopulations and might circumvent the possibility that some differentiated tumor cells can dedifferentiate and repopulate the stem cell fraction (58). Another potential complication of cancer stem cell–directed therapies is that nonneoplastic stem cells may also be depleted by such strategies. This is of particular concern in children who will presumably require stem cells for the maintenance and repair of a host of tissues over the course of their lives. Of note, we found that i.p. injections of GSI-18 for 5 days blocked tumor formation with no obvious ill effects on the animal's health over the subsequent months. Indeed, it has recently been shown that inhibition of γ-secretase activity using small-molecule drugs can actually enhance long-term memory in rodents (59).

In summary, we show that in the malignant brain tumor medulloblastoma, Notch pathway blockade depletes a population of cells required for *in vivo* tumor formation by suppressing

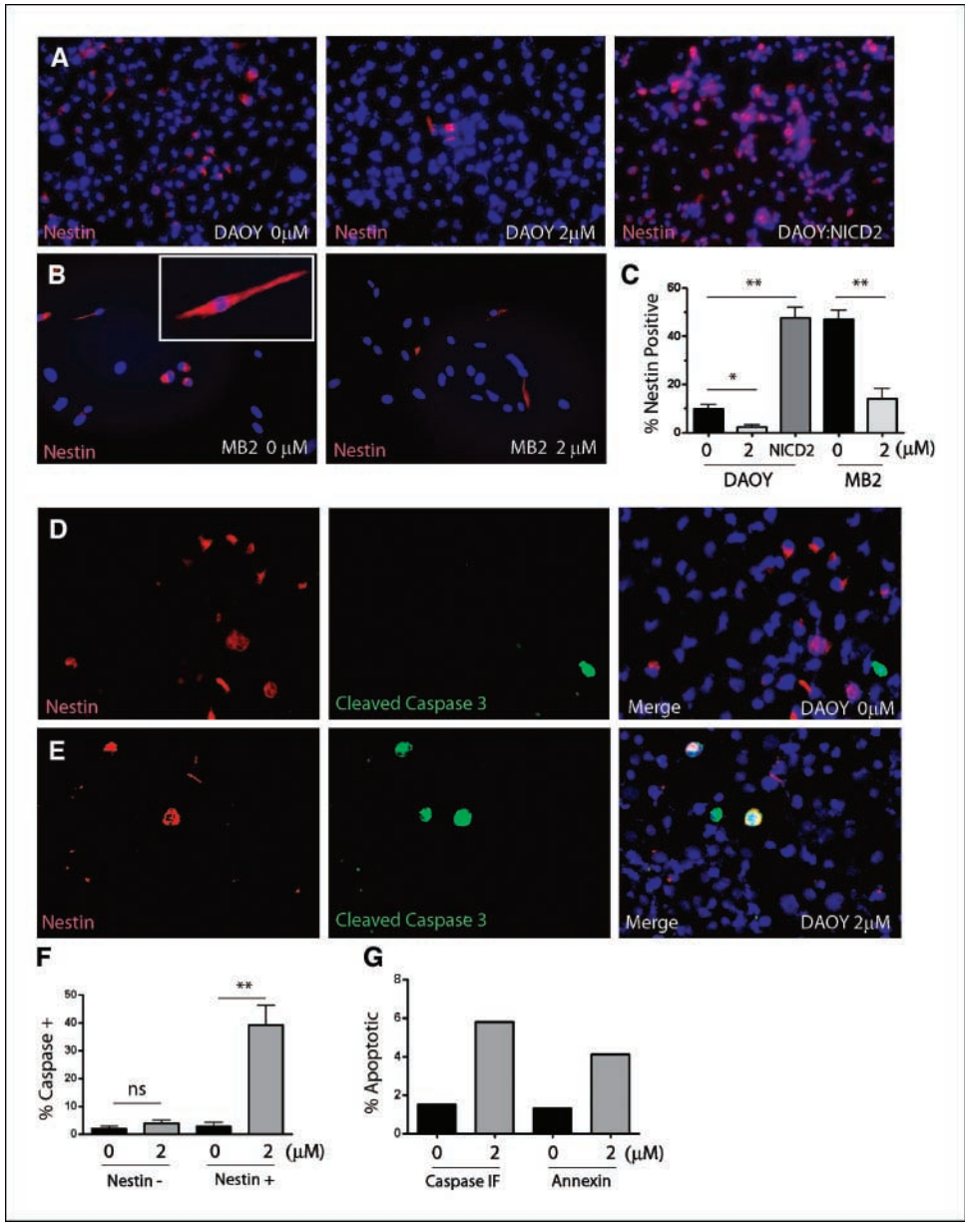

Figure 6. Nestin-positive cells are especially sensitive to Notch pathway blockade. *A,* the fraction of DAOY cells expressing high levels of nestin is lower after GSI-18 exposure and higher in a subclone expressing activated Notch2 (NICD2). *B* and *C,* similar effects are seen following Notch blockade in the low-passage medulloblastoma cell line MB2. *D* to *F,* double immunolabeling was used assess both differentiation status (nestin) and apoptosis (cleaved caspase-3) in DAOY cultures. Significant induction of cleaved caspase-3–positive apoptotic cells following Notch blockade was limited to the nestin-positive subpopulation. *G,* overall apoptotic induction in DAOY cultures was similar when measured by counts of cleaved caspase-3 immunofluorescent (*IF*) cells or flow cytometric analysis of Annexin. *, $P < 0.01$; ** P, < 0.001 (*t* tests); *ns,* not significant.

proliferation and inducing apoptosis or differentiation in stem-like cells. Our data suggest that Notch pathway blockers may be the first of a new class of chemotherapeutic agents—those targeting cancer stem cells.

Acknowledgments

Received 3/13/2006; revised 5/17/2006; accepted 5/25/2006.

Grant support: Alzheimer's Association, Zenith Fellowship (Y-M. Li), NIH grant 1R01AG026660-01, The Children's Cancer Foundation of Baltimore, Fellowship from the American Brain Tumor Association (X. Fan), Burroughs Wellcome Fund Career Award in the Biomedical Sciences (C.G. Eberhart), and NIH grant K08 NS43279.

The costs of publication of this article were defrayed in part by the payment of page charges. This article must therefore be hereby marked *advertisement* in accordance with 18 U.S.C. Section 1734 solely to indicate this fact.

We thank Josh Copeland for assistance with Western blots, Dr. Tetsuo Sudo for his generous gift of Hes1 antiserum, and Dr. J.C. Zuniga-Pflucker for his suggestions on Notch inhibition and cell size.

References

1. Kleihues P, Cavenee W. Tumors of the nervous system. Lyon (France): IARC Press; 2000.
2. Oliver TG, Wechsler-Reya RJ. Getting at the root and stem of brain tumors. Neuron 2004;42:885–8.
3. Rorke LB. The cerebellar medulloblastoma and its relationship to primitive neuroectodermal tumors. J Neuropathol Exp Neurol 1983;42:1–15.
4. Raffel C, Jenkins RB, Frederick L, et al. Sporadic medulloblastomas contain PTCH mutations. Cancer Res 1997;57:842–5.
5. Reifenberger J, Wolter M, Weber RG, et al. Missense mutations in SMOH in sporadic basal cell carcinomas of the skin and primitive neuroectodermal tumors of the central nervous system. Cancer Res 1998;58:1798–803.
6. Eberhart CG, Tihan T, Burger PC. Nuclear localization and mutation of β-catenin in medulloblastomas. J Neuropathol Exp Neurol 2000;59:333–7.
7. Zurawel RH, Chiappa SA, Allen C, Raffel C. Sporadic medulloblastomas contain oncogenic β-catenin mutations. Cancer Res 1998;58:896–9.
8. Fan X, Mikolaenko I, Elhassan I, et al. Notch1 and notch2 have opposite effects on embryonal brain tumor growth. Cancer Res 2004;64:7787–93.
9. Hallahan AR, Pritchard JI, Hansen S, et al. The SmoA1 mouse model reveals that notch signaling is critical for the growth and survival of sonic hedgehog-induced medulloblastomas. Cancer Res 2004;64:7794–800.
10. Berman DM, Karhadkar SS, Hallahan AR, et al. Medulloblastoma growth inhibition by hedgehog pathway blockade. Science 2002;297:1559–61.
11. Romer JT, Kimura H, Magdaleno S, et al. Suppression of the Shh pathway using a small molecule inhibitor eliminates medulloblastoma in Ptc1(+/−)p53(−/−) mice. Cancer Cell 2004;6:229–40.
12. Sanchez P, Ruiz IAA. *In vivo* inhibition of endogenous brain tumors through systemic interference of Hedgehog signaling in mice. Mech Dev 2005;122:223–30.
13. Gilbertson RJ. Medulloblastoma: signalling a change in treatment. Lancet Oncol 2004;5:209–18.
14. Romer J, Curran T. Targeting medulloblastoma: small-molecule inhibitors of the Sonic Hedgehog pathway as potential cancer therapeutics. Cancer Res 2005;65:4975–8.
15. Rood BR, Macdonald TJ, Packer RJ. Current treatment of medulloblastoma: recent advances and future challenges. Semin Oncol 2004;31:666–75.
16. Singh SK, Clarke ID, Hide T, Dirks PB. Cancer stem cells in nervous system tumors. Oncogene 2004;23:7267–73.
17. Wang JC, Dick JE. Cancer stem cells: lessons from leukemia. Trends Cell Biol 2005;15:494–501.
18. Huntly BJ, Gilliland DG. Leukaemia stem cells and the evolution of cancer-stem-cell research. Nat Rev Cancer 2005;5:311–21.
19. Park CH, Bergsagel DE, McCulloch EA. Mouse myeloma tumor stem cells: a primary cell culture assay. J Natl Cancer Inst 1971;46:411–22.
20. Bruce WR, Van Der Gaag H. A quantitative assay for the number of murine lymphoma cells capable of proliferation *in vivo*. Nature 1963;199:79–80.
21. Hamburger AW, Salmon SE. Primary bioassay of human tumor stem cells. Science 1977;197:461–3.
22. Bonnet D, Dick JE. Human acute myeloid leukemia is organized as a hierarchy that originates from a primitive hematopoietic cell. Nat Med 1997;3:730–7.
23. Lapidot T, Sirard C, Vormoor J, et al. A cell initiating human acute myeloid leukaemia after transplantation into SCID mice. Nature 1994;367:645–8.
24. Singh SK, Hawkins C, Clarke ID, et al. Identification of human brain tumour initiating cells. Nature 2004;432:396–401.
25. Kondo T, Setoguchi T, Taga T. Persistence of a small subpopulation of cancer stem-like cells in the C6 glioma cell line. Proc Natl Acad Sci U S A 2004;101:781–6.
26. Patrawala L, Calhoun T, Schneider-Broussard R, Zhou J, Claypool K, Tang DG. Side population is enriched in tumorigenic, stem-like cancer cells, whereas ABCG2+ and ABCG2− cancer cells are similarly tumorigenic. Cancer Res 2005;65:6207–19.
27. Taylor MD, Poppleton H, Fuller C, et al. Radial glia cells are candidate stem cells of ependymoma. Cancer Cell 2005;8:323–35.
28. Goodell MA, Brose K, Paradis G, Conner AS, Mulligan RC. Isolation and functional properties of murine hematopoietic stem cells that are replicating *in vivo*. J Exp Med 1996;183:1797–806.
29. Uchida N, Buck DW, He D, et al. Direct isolation of human central nervous system stem cells. Proc Natl Acad Sci U S A 2000;97:14720–5.
30. Miraglia S, Godfrey W, Yin AH, et al. A novel five-transmembrane hematopoietic stem cell antigen: isolation, characterization, and molecular cloning. Blood 1997;90:5013–21.
31. Yin AH, Miraglia S, Zanjani ED, et al. AC133, a novel marker for human hematopoietic stem and progenitor cells. Blood 1997;90:5002–12.
32. Hemmati HD, Nakano I, Lazareff JA, et al. Cancerous stem cells can arise from pediatric brain tumors. Proc Natl Acad Sci U S A 2003;100:15178–83.
33. Singh SK, Clarke ID, Terasaki M, et al. Identification of a cancer stem cell in human brain tumors. Cancer Res 2003;63:5821–8.
34. Galli R, Binda E, Orfanelli U, et al. Isolation and characterization of tumorigenic, stem-like neural precursors from human glioblastoma. Cancer Res 2004;64:7011–21.
35. Reya T, Morrison SJ, Clarke MF, Weissman IL. Stem cells, cancer, and cancer stem cells. Nature 2001;414:105–11.
36. Solecki DJ, Liu XL, Tomoda T, Fang Y, Hatten ME. Activated Notch2 signaling inhibits differentiation of cerebellar granule neuron precursors by maintaining proliferation. Neuron 2001;31:557–68.
37. Gaiano N, Fishell G. The role of notch in promoting glial and neural stem cell fates. Annu Rev Neurosci 2002;25:471–90.
38. Weng AP, Ferrando AA, Lee W, et al. Activating mutations of NOTCH1 in human T cell acute lymphoblastic leukemia. Science 2004;306:269–71.
39. Lewis SJ, Smith AL, Neduvelil JG, et al. A novel series of potent γ-secretase inhibitors based on a benzobicyclo[4.2.1]nonane core. Bioorg Med Chem Lett 2005;15:373–8.
40. Li YM, Lai MT, Xu M, et al. Presenilin 1 is linked with γ-secretase activity in the detergent solubilized state. Proc Natl Acad Sci U S A 2000;97:6138–43.
41. Ciofani M, Zuniga-Pflucker JC. Notch promotes survival of pre-T cells at the β-selection checkpoint by regulating cellular metabolism. Nat Immunol 2005;6:881–8.
42. Ishibashi M, Ang SL, Shiota K, Nakanishi S, Kageyama R, Guillemot F. Targeted disruption of mammalian hairy and Enhancer of split homolog-1 (HES-1) leads to up-regulation of neural helix-loop-helix factors, premature neurogenesis, and severe neural tube defects. Genes Dev 1995;9:3136–48.
43. van Es JH, van Gijn ME, Riccio O, et al. Notch/γ-secretase inhibition turns proliferative cells in intestinal crypts and adenomas into goblet cells. Nature 2005;435:959–63.
44. Kato K. Novel GABAA receptor α subunit is expressed only in cerebellar granule cells. J Mol Biol 1990;214:619–24.
45. Lee A, Kessler JD, Read TA, et al. Isolation of neural stem cells from the postnatal cerebellum. Nat Neurosci 2005;8:723–9.
46. Lendahl U, Zimmerman LB, McKay RD. CNS stem cells express a new class of intermediate filament protein. Cell 1990;60:585–95.
47. Sahlgren CM, Mikhailov A, Hellman J, et al. Mitotic reorganization of the intermediate filament protein nestin involves phosphorylation by cdc2 kinase. J Biol Chem 2001;276:16456–63.
48. Wulf GG, Wang RY, Kuehnle I, et al. A leukemic stem cell with intrinsic drug efflux capacity in acute myeloid leukemia. Blood 2001;98:1166–73.
49. Dean M, Fojo T, Bates S. Tumour stem cells and drug resistance. Nat Rev Cancer 2005;5:275–84.
50. Donnenberg VS, Donnenberg AD. Multiple drug resistance in cancer revisited: the cancer stem cell hypothesis. J Clin Pharmacol 2005;45:872–7.
51. Hirschmann-Jax C, Foster AE, Wulf GG, et al. A distinct "side population" of cells with high drug efflux capacity in human tumor cells. Proc Natl Acad Sci U S A 2004;101:14228–33.
52. Weng AP, Aster JC. Multiple niches for Notch in cancer: context is everything. Curr Opin Genet Dev 2004;14:48–54.
53. Radtke F, Raj K. The role of Notch in tumorigenesis: oncogene or tumour suppressor? Nat Rev Cancer 2003;3:756–67.
54. Dang TP, Gazdar AF, Virmani AK, et al. Chromosome 19 translocation, overexpression of Notch3, and human lung cancer. J Natl Cancer Inst 2000;92:1355–7.
55. Pece S, Serresi M, Santolini E, et al. Loss of negative regulation by Numb over Notch is relevant to human breast carcinogenesis. J Cell Biol 2004;167:215–21.
56. Tonon G, Modi S, Wu L, et al. t(11;19)(q21;p13) translocation in mucoepidermoid carcinoma creates a novel fusion product that disrupts a Notch signaling pathway. Nat Genet 2003;33:208–13.
57. Miyamoto Y, Maitra A, Ghosh B, et al. Notch mediates TGFα-induced changes in epithelial differentiation during pancreatic tumorigenesis. Cancer Cell 2003;3:565–76.
58. Fomchenko EI, Holland EC. Stem cells and brain cancer. Exp Cell Res 2005;306:323–9.
59. Dash PK, Moore AN, Orsi SA. Blockade of γ-secretase activity within the hippocampus enhances long-term memory. Biochem Biophys Res Commun 2005;338:777–82.